VI International Conference on Computational Methods for Coupled Problems in Science and Engineering
COUPLED PROBLEMS 2015
B. Schrefler, E. Oñate and M. Papadrakakis(Eds)

TOWARDS GOAL-ORIENTED MESH ADAPTATION FOR FLUID-STRUCTURE INTERACTION

E. GAUCI[a], F. ALAUZET[b], A. LOSEILLE[b], A.DERVIEUX[a]

[a] INRIA, Projet Ecuador, 2004 route des Lucioles - BP 93, 06902 Sophia Antipolis, France

[b] INRIA, Projet Gamma, Domaine de Voluceau, Rocquencourt, BP 105, 78153 Le Chesnay, France.

Key words: Unsteady compressible flow, Arbitrary Lagrangian Eulerian, goal-oriented mesh adaptation, anisotropic mesh adaptation, adjoint, metric.

Abstract. In order to address fluid-structure interaction, we present an *a priori* analysis for an ALE compressible flow model. This analysis is the key for an anisotropic metric-based mesh adaptation.

1 INTRODUCTION

This work takes place into a serie of works for metric-based goal-oriented mesh adaptation. Metrics are matrix fields representing a mesh thanks to the description of three (3D case) or two (2D) orthogonal vectors giving the directions of stretching of the mesh associated with the definition of the mesh size in each directions. In anisotropic mesh adaptation, the optimal metric has to be derived from the minimization of a model of the approximation error. Historically, the first model was a linear interpolation error model, leading to the so-called Hessian-based anisotropic adaptation. The optimal metric field, *i.e.* the optimal sizes and orientations distribution that will be used to govern the generation of the new mesh, is obtained as the solution of the problem of minimization of the global interpolation error. It thus depends on a computed solution, but the link with the original PDE is sometimes too weak. In contrast, goal-oriented mesh adaptation takes into account the PDE, via the introduction of an adjoint state. Extension of goal-oriented analysis to anisotropic mesh adaptation has been proposed in [15] and [11] for the steady Euler equations. An extension to transient Euler with the design of a global transient global fixed point (TFP) mesh adaptation algorithm was proposed in [7]. The TFP computes the n meshes to be used in the N_i time sub-intervals of the global time interval $]0, T[$ of the simulation. To generate the N_i sub-interval meshes, the complete state solution from time 0 to time T must first be computed as long as the complete adjoint solution from T to 0.

In order to be able, in the long term, to address fluid-structure interaction, the metric-based adaptation needs to be extended to Arbitrary-Lagrangian-Eulerian (ALE) formulations. In ALE, the mesh is moving (in fact deforming) during any time interval. An important and difficult issue is to force the mesh to stay optimally adapted while moving. In the case of a Hessian-based adaptation, the mesh needs to be adapted at any time to a time-dependent criterion, the Hessian of the unsteady sensor. But the mesh is also uniquely defined by the initial mesh and the prescribed ALE mapping. In [5, 4], the two constraints are simultaneously respected by (1) for any time mapping adaptation constraints on the initial mesh, and then (2) taking the metric-intersection of these constraints on the initial mesh. The resulting ALE-TFP adaptation has been successfully applied to several fluid-structure interaction computations. Although very efficient, this method is a Hessian-based one and inherits the Hessian-based deficiencies, which involves, as already pointed out, an insufficient accounting of the PDE itself. The purpose of the work reported here is to extend the goal-oriented formulation of [11][7] to ALE calculations. In other words, we try to build a metric-based, goal-oriented unsteady anisotropic mesh adaptation method for an ALE Euler model. In the present short paper, we concentrate on the ALE error analysis for a given time-step.

2 CONTINUOUS MESH MODEL

We propose to work in the continuous mesh framework, introduced in [9, 10]. The main idea of this framework is to model continuously discrete meshes by Riemannian metric spaces. This enables to define proper differentiable optimization [2, 6], *i.e.,* to use calculus of variations on continuous meshes. Indeed, trying to solve optimality problems manipulating discrete meshes generally leads to intractable problems in practice. This framework lies in the class of metric-based methods. A continuous mesh $\mathcal{M}$ of computational domain Ω is identified to a Riemannian metric field [8] $\mathcal{M} = (\mathcal{M}(\mathbf{x}))_{\mathbf{x}\in\Omega}$. For all $\mathbf{x}$ of Ω, $\mathcal{M}(\mathbf{x})$ is a symmetric 3×3 matrix having $(\lambda_i(\mathbf{x}))_{i=1,3}$ as positive eigenvalues along the principal directions $\mathcal{R}(\mathbf{x}) = (\mathbf{v}_i(\mathbf{x}))_{i=1,3}$. Sizes along these directions are denoted $(h_i(\mathbf{x}))_{i=1,3} = (1/\sqrt{\lambda_i}(\mathbf{x}))_{\mathbf{i=1,3}}$ and the three *anisotropy quotients* r_i are defined as: $r_i = h_i^3\,(h_1h_2h_3)^{-1}$. The diagonalization of $\mathcal{M}(\mathbf{x})$ writes:

$$\mathcal{M}(\mathbf{x}) = \sqrt[3]{\det(\mathcal{M})}(\mathbf{x})\,\mathcal{R}(\mathbf{x})\mathrm{Diag}(r_1^{-\frac{2}{3}}(\mathbf{x}), r_2^{-\frac{2}{3}}(\mathbf{x}), r_3^{-\frac{2}{3}}(\mathbf{x}))^t\mathcal{R}(\mathbf{x}), \tag{1}$$

The *complexity* $\mathcal{C}$ of a continuous mesh is the continuous counterpart of the total number of vertices:

$$\mathcal{C}(\mathcal{M}) = \int_\Omega \sqrt{\det(\mathcal{M}(\mathbf{x}))}\,\mathrm{d}\mathbf{x}.$$

Given a continuous mesh $\mathcal{M}$, we shall say, following [9, 10], that a discrete mesh $\mathcal{H}$ of the same domain Ω is a unit mesh with respect to $\mathcal{M}$, if each tetrahedron $K\in\mathcal{H}$, defined by its list of edges $(\mathbf{e}_i)_{i=1\ldots6}$, verifies:

$$\forall i\in[1,6],\quad \ell_{\mathcal{M}}(\mathbf{e}_i)\in\left[\frac{1}{\sqrt{2}},\sqrt{2}\right],\ \text{in which}\ \ell_{\mathcal{M}}(\mathbf{ab}) = \int_0^1 \sqrt{{}^t\mathbf{ab}\,\mathcal{M}(\mathbf{a}+t\,\mathbf{ab})\,\mathbf{ab}}\,\mathrm{d}t.$$

Given a smooth function u, each unit mesh $\mathcal{H}$ with respect to $\mathcal{M}$ is associated with a local interpolation error $|u - \Pi_{\mathcal{H}} u|$. In [9, 10], it is shown that all these interpolation errors are well represented by the so-called continuous interpolation error related to $\mathcal{M}$, which is expressed locally in terms of the Hessian H_u of u as follows:

$$(u - \pi_{\mathcal{M}} u)(\mathbf{x}, t) \quad = \quad \frac{1}{10} \text{trace}(\mathcal{M}^{-\frac{1}{2}}(\mathbf{x}) \, |H_u(\mathbf{x}, t)| \, \mathcal{M}^{-\frac{1}{2}}(\mathbf{x}))$$

where $|H_u|$ is deduced from the Hessian H_u of u by taking the absolute values of its eigenvalues and where time-dependency notations have been added for use in the next sections.

3 ALE EULER MODEL

ALE domain and functions. Let Ω_0 be a smooth domain of $\mathbb{R}^d$. For any t in $]0, T[$ we have a mapping: $\boldsymbol{\phi} : \Omega_0 \times]0, T[\to \mathbb{R}^d$ satisfying: $\boldsymbol{\phi}(x, 0) = x$ and for which we assume that there exists a smooth deformation velocity $\dot{\boldsymbol{\phi}} = \partial \boldsymbol{\phi} / \partial t$. Let $\Omega_t = \boldsymbol{\phi}(\Omega_0, t)$.

We call Q_T the non-cylindrical union of all Ω_t for t in $]0, T[$:

$$Q_T = \bigcup_{t=0}^{t=T} \boldsymbol{\phi}(\Omega_0, t).$$

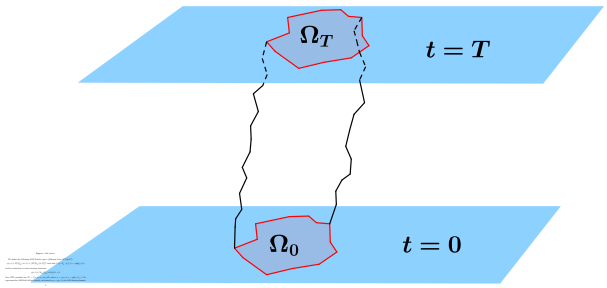

pressure, and $E = E(x,t)$ the ALE energy per unit mass. u, v, and w are the ALE Cartesian components of the ALE velocity vector $\mathbf{u}$.

The ALE-Euler fluxes write :

$$\mathcal{F}(W) = {}^t(\rho,\ \rho(\mathbf{u}-\dot{\boldsymbol{\phi}})u + p\mathbf{e}_x,\ \rho(\mathbf{u}-\dot{\boldsymbol{\phi}})v + p\mathbf{e}_y,\ \rho(\mathbf{u}-\dot{\boldsymbol{\phi}})w + p\mathbf{e}_z,\ \rho(\mathbf{u}-\dot{\boldsymbol{\phi}})E + \mathbf{u}p).$$

Let us define the variational formulation of the ALE-Euler system:

$$\text{Find } W \in \mathcal{H}^1(Q_T) \text{ such that } \forall \varphi \in \mathcal{H}^1_{cst}(Q_T), \quad (\Psi(W)\,,\,\varphi) = 0$$

$$\begin{aligned}\text{with} \quad (\Psi(W)\,,\,\varphi) \;&=\; \int_{\Omega_0} \varphi(0)(W_0 - W(0))\,\mathrm{d}\Omega \;+\; \int_0^T \frac{\partial}{\partial t}\int_{\Omega_t} \varphi W\,\mathrm{d}\Omega\,\mathrm{d}t \\ &+\; \int_0^T\int_{\Omega_t} \varphi\,\nabla\cdot\mathcal{F}(W)\,\mathrm{d}\Omega\,\mathrm{d}t \;-\; \int_0^T\int_{\partial\Omega_t} \varphi\,\hat{\mathcal{F}}(W).\mathbf{n}\,\mathrm{d}\Gamma\,\mathrm{d}t\,, \quad (2)\end{aligned}$$

where $\hat{\mathcal{F}}$ takes into account the boundary conditions. Note that the ∇ is a differentiation for constant time, identifying x-derivative and ξ-derivatives.

Time-discretized formulation. The ALE-Euler model will be advanced in time by an explicit scheme. For simplicity, we write it as a Forward-Euler time advancing:

$$\begin{aligned}&\text{Find } W \in \mathcal{H}^1(Q_T) \text{ such that } \forall \varphi \in \mathcal{H}^1_{cst}(Q_T), \quad (\Psi(W)\,,\,\varphi) = 0 \ \text{ with} \\ &(\Psi(W)\,,\,\varphi) = \int_{\Omega_0} \varphi(0)(W_0 - W^1)\,\mathrm{d}\Omega \\ &+ \sum_{n=1}^{nmax} \frac{1}{t^{n+1}-t^n}\left[\int_{\Omega_{t^{n+1}}} \varphi(.,t^{n+1})W(.,t^{n+1})\,\mathrm{d}\Omega - \int_{\Omega_{t^n}} \varphi(.,t^n)W(.,t^n)\,\mathrm{d}\Omega\right] \\ &+ \sum_{n=1}^{nmax}\int_{\Omega_{tn}} \varphi(.,t^n)\,\nabla\cdot\mathcal{F}(W(.,t^n))\,\mathrm{d}\Omega - \sum_{n=1}^{nmax}\int_{\partial\Omega_{tn}} \varphi(.,t^n)\,\hat{\mathcal{F}}(W(.,t^n)).\mathbf{n}\,\mathrm{d}\Gamma. \quad (3)\end{aligned}$$

For the sake of simplicity again, we shall not address the time discretization error in this paper. Some justification of this option for explicit time advancing can be found in [3].

Fully discrete formulation. Let us consider τ_h a finite-element triangulation (2D) or tetrahedrization (3D) of Ω. We assume that $\Omega_h^n = \Omega^n$. We consider a dual finite-volume tessellation made of median-limited cells:

$$\Omega_h^n = \bigcup_{elements} T_h = \bigcup_{ic,cells} cell_h(ic)$$

We define the following approximation space derived from the standard P_1 FEM approximation space :

$$\begin{aligned}\mathcal{V}_h \;=\; &\{\varphi \in \mathcal{H}^1(Q_T),\ \ \varphi \in \mathcal{C}^0(\bar{Q}_t),\\ &\forall\ t \in]0,T[,\ \forall \text{ element } T \in \tau_h, \varphi(.,t)|_T \text{ is affine}\\ &\forall\ n,\ 1 \le nmax,\ \forall\ i \text{ vertex} \in \tau_h,\ \varphi(\mathbf{x}(i),.) \text{ is affine in time}\}.\end{aligned}$$

We define $\mathcal{V}_{h,cst} = \mathcal{H}^1_{cst}(Q_T) \cap \mathcal{V}_h$ and the interpolation operator:

$$\Pi_h : \mathcal{H}^1(Q_T) \to \mathcal{V}_h \ \ ; \ \ \Pi_h\varphi(\mathbf{x}(i), t^n) = \varphi(\mathbf{x}(i), t^n) \ \forall \ i \text{ vertex}, \ \forall \ n, \ 1 \leq nmax.$$

The fully discrete state system which we consider (similarly to [11]) writes:

$$\text{Find } W_h \in \mathcal{V}_h \text{ such that } \forall \varphi_h \in \mathcal{V}_{h,cst}, \quad (\Psi_h(W_h) \, , \, \varphi_h) = 0 \tag{4}$$

with $\quad \forall W \in \mathcal{H}^1(Q_T), \forall \varphi \in \mathcal{H}^1(Q_T) \, ,$

$$(\Psi_h(W) \, , \, \varphi) = \int_{\Omega_0} \varphi(., t^1)(\Pi_h W_0 - \Pi_h W(., t^1)) \, \mathrm{d}\Omega$$
$$+ \sum_{n=1}^{nmax} \frac{1}{t^{n+1} - t^n} \left[\int_{\Omega_{t^{n+1}}} \Pi_h\varphi(., t^{n+1}) \Pi_h W(., t^{n+1}) \, \mathrm{d}\Omega \ - \ \int_{\Omega_{t^n}} \Pi_h\varphi(., t^n) \Pi_h W(., t^n)) \, \mathrm{d}\Omega \right]$$
$$+ \sum_{n=1}^{nmax} \int_{\Omega_{t^n}} \Pi_h\varphi(., t^n)) \, \nabla \cdot \Pi_h \mathcal{F}(W(., t^n))) \, \mathrm{d}\Omega - \sum_{n=1}^{nmax} \int_{\partial\Omega_{t^n}} \Pi_h\varphi(., t^n)) \, \Pi_h \hat{\mathcal{F}}(W(., t^n)).\mathbf{n} \, \mathrm{d}\Gamma$$

The Π_h in the initial condition and time derivative are useless for the discrete equation statement, but essential for the extension of the discrete residual to continuous functions of $\mathcal{H}^1(Q_T)$. Note that if in these initial and time terms the interpolation operator is replaced by a projection P_0 onto functions which are constant by cells, we get:

$$\int_{\Omega_{t^{n+1}}} P_0\varphi P_0 W^{n+1} \, \mathrm{d}\Omega \, \mathrm{d}t - \int_{\Omega_{t^n}} P_0\varphi P_0 W^n \, \mathrm{d}\Omega \, \mathrm{d}t \ =$$
$$\sum_{cells,ic} \varphi(ic) \left(|meas(ic)^{n+1}| W^{n+1}(ic) - |meas(ic)^n| W^n(ic) \right)$$

in which we recognize the usual ALE finite-volume time-derivative.

4 MESH ADAPTATION HESSIAN-BASED CRITERION

4.1 Instantaneous mesh adaptation criterion

Let $s(W)$ a sensor function computed from the CFD field W at time t. It can be for example the corresponding Mach number. Starting from:

$$\|s(W) - \pi_{\mathcal{M}} s(W)\|_{\mathbf{L}^p(\Omega_h)} = \left(\int_\Omega \left(\mathrm{trace}\big(\mathcal{M}^{-\frac{1}{2}}(\mathbf{x}) |H_{s(W)}(\mathbf{x})| \mathcal{M}^{-\frac{1}{2}}(\mathbf{x}) \big) \right)^p \mathrm{d}\mathbf{x} \right)^{\frac{1}{p}} \tag{5}$$

we define as optimal metric the one which minimizes the right hand side under the constraint of a total number of vertices equal to a parameter N. After solving analytically this optimization problem, we get the unique optimal $(\mathcal{M}_{\mathbf{L}^p}(\mathbf{x}))_{\mathbf{x}\in\Omega}$ as:

$$\mathcal{M}_{\mathbf{L}^p} = D_{\mathbf{L}^p} \left(\det \left| H_{s(W)} \right| \right)^{\frac{-1}{2p+2}} |H_{s(W)} u| \ \text{ and } \ D_{\mathbf{L}^p} = N \left(\int_\Omega (\det \left| H_{s(W)} \right|)^{\frac{p}{2p+2}} \right)^{-1}, \tag{6}$$

where $D_{\mathbf{L}^p}$ is a global normalization term set to obtain a continuous mesh with complexity N and $(\det|H_u|)^{\frac{-1}{2p+2}}$ is a local normalization term accounting for the sensitivity of the $\mathbf{L}^p$ norm. In the case of an adaptation loop for solving a Partial Differential Equation, a continuous sensor function $s(W)$ is not available, but an approximate solution $s(W_{\mathcal{M}})$. In that case, the continuous interpolation error (2) is replaced by:

$$|s(W_{\mathcal{M}}) - \pi_{\mathcal{M}} s(W_{\mathcal{M}})|(\mathbf{x}) \;=\; \frac{1}{10}\text{trace}(\mathcal{M}^{-\frac{1}{2}}(\mathbf{x})\,|H_{s(W_{\mathcal{M}})}(\mathbf{x})|\,\mathcal{M}^{-\frac{1}{2}}(\mathbf{x})) \tag{7}$$

where $H_{s(W_{\mathcal{M}})}$ is an approximate Hessian of the discrete sensor, which is evaluated by the patch-recovery approximation defined in [14]. According to the continuous mesh framework, statement (6) defines directly a continuous optimal metric. In practice, solving (6) is done by approximation, *i.e.* in a discrete context with a couple (mesh, solution) denoted $(\mathcal{H}_{\mathcal{M}}, W_{\mathcal{M}})$ and iteratively through the following fixed point:

Step 1: compute the discrete state $W_{\mathcal{M}}$ on mesh $\mathcal{H}_{\mathcal{M}}$,
Step 2: compute sensor $s_{\mathcal{M}} = s(u_{\mathcal{M}})$ and optimal metric $\mathcal{M}^{opt}_{inter} = \mathcal{K}_p(H_{\mathcal{M}}(s_{\mathcal{M}}))$
Step 3: $\mathcal{M} = \mathcal{M}^{opt}_{inter}$, $\mathcal{H}_{\mathcal{M}} = \mathcal{H}_{\mathcal{M}^{opt}_{inter}}$ and go to step 1, until convergence.

4.2 A numerical example

The above method gives an optimal metric for each time of $[0, T]$. In practice, the global interval $[0, T]$ is divided into sub-intervals, $[0, T] = \cup[t_p, t_{p+1}]$ on which meshes will keep a constant topology. At each time level t^n inside $[t_p, t_{p+1}]$, we have (6) an optimal metric which is also a specification of the maximal mesh size in each direction for controlling the error to a prescribed level. This specification for t^n is therefore a constraint which we map onto the first mesh at time t_p of the subinterval. To take into account the different constraints for the different t^n of $[t_p, t_{p+1}]$, an intersection of these metrics is performed, defining the metric and the mesh at t_p, insuring that deformed mesh in $[t_p, t_{p+1}]$ satisfies the adaptation constraint. An example of computation deals with the 2D fluid-structure interaction due to the impact of a blast wave on a mobile rigid rectangular mass, cf. Figure 2.

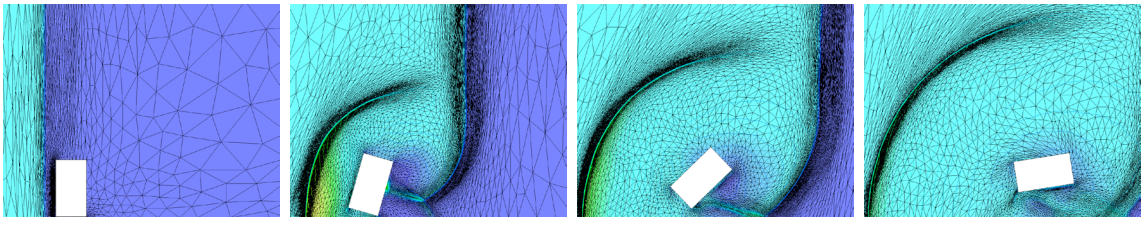

Figure 2: Application of the Fixed-Point algorithm to a blast wave inpinging an obstacle.

5 MESH ADAPTATION GOAL-ORIENTED CRITERION

According to the goal-oriented paradigm, we introduce two scalar outputs depending of the state variables (W and W_h are respectively the solutions of (3) and (5)):

$$j(W) = (g, W)_{L^2(Q_T)} \quad ; \quad \delta j = j(W) - j(W_h)$$

and we are interested by minimizing the approximation error committed on the evaluation δj of j. Following [11], [7], we formally develop δj with the help of the continuous and discrete adjoint states:

$$W^* \in \mathcal{V}, \forall \psi \in \mathcal{V}, \quad \left(\frac{\partial \Psi}{\partial W}(W)\psi, W^* \right) = (g, \psi), \tag{8}$$

$$W_h^* \in \mathcal{V}_h, \forall \psi_h \in \mathcal{V}_h, \quad \left(\frac{\partial \Psi_h}{\partial W}(W_h)\psi_h, W_h^* \right) = (g, \psi_h). \tag{9}$$

The idea is now to compute the difference of variational residual for a discrete test function:

$$(\Psi_h(W), \varphi_h) - (\Psi_h(W_h), \varphi_h) = (\Psi_h(W) - \Psi(W), \varphi_h)$$

Then assuming that W^*, $\Pi_h W^*$ and W_h^* and their gradients are close to each other:

$$\delta j \approx (\Psi_h(W) - \Psi(W), W^*) \approx (\Psi_h(W) - \Psi(W), \Pi_h W^*)\,. \tag{10}$$

The term $\Psi_h(W) - \Psi(W)$ is an *a posteriori* local error which we now evaluate.

5.1 Local error analysis

We replace in Estimation (10) operators Ψ and Ψ_h by their expressions given by Relations (3) and (5). We follow again this option. We also discard the error committed when imposing the initial condition. We finally get the following simplified error model:

$$\begin{aligned}
\delta j \approx & \sum_{n=1}^{n=nmax} \frac{1}{t^{n+1} - t^n} \int_{\Omega_{t^{n+1}}} \Pi_h W^{*,n+1} (\Pi_h W^{n+1} - W^{n+1})\, \mathrm{d}\Omega \\
& - \sum_{n=1}^{n=nmax} \frac{1}{t^{n+1} - t^n} \int_{\Omega_{t^n}} \Pi_h W^{*,n} (\Pi_h W^n) - W^n)\, \mathrm{d}\Omega \\
& + \sum_{n=1}^{n=nmax} \int_{\Omega_{t^n}} \Pi_h W^{*,n}\, \nabla \cdot (\Pi_h \mathcal{F}(W^n) - \mathcal{F}(W^n))\, \mathrm{d}\Omega \\
& - \sum_{n=1}^{n=nmax} \int_{\partial\Omega_{t^n}} \Pi_h W^{*,n}\, (\Pi_h \hat{\mathcal{F}}(W^n) - \hat{\mathcal{F}}(W^n)).\mathbf{n}\, \mathrm{d}\Gamma.
\end{aligned} \tag{11}$$

Integrating by parts leads to:

$$\begin{aligned}
\delta j \;\approx\; & \sum_{n=1}^{n=nmax} \frac{1}{t^{n+1}-t^n} \int_{\Omega_{t^{n+1}}} \Pi_h W^{*,n+1}(\Pi_h W^{n+1} - W^{n+1})\,\mathrm{d}\Omega \\
- & \sum_{n=1}^{n=nmax} \frac{1}{t^{n+1}-t^n} \int_{\Omega_{t^n}} \Pi_h W^{*,n}(\Pi_h W^n) - W^n)\,\mathrm{d}\Omega \\
- & \sum_{n=1}^{n=nmax} \int_{\Omega_{t^n}} \nabla \Pi_h W^{*,n} \cdot (\Pi_h \mathcal{F}(W^n) - \mathcal{F}(W^n))\,\mathrm{d}\Omega \\
- & \sum_{n=1}^{n=nmax} \int_{\partial\Omega_{t^n}} \Pi_h W^{*,n}\,(\Pi_h \bar{\mathcal{F}}(W^n) - \bar{\mathcal{F}}(W^n)).\mathbf{n}\,\mathrm{d}\Gamma. \qquad (12)
\end{aligned}$$

with $\bar{\mathcal{F}} = \hat{\mathcal{F}} - \mathcal{F}$. We observe that this estimate of δj is expressed in terms of interpolation errors of the Euler fluxes and of the time derivative weighted by continuous functions $\Pi_h W^* \approx W^*$ and $\nabla \Pi_h W^* \approx \nabla W^*$. The integrands in Error Estimation (12) contain positive and negative parts which can compensate for some particular meshes. In our strategy, we prefer not to rely on these parasitic effects and to slightly over-estimate the error. To this end, all integrands are bounded by their absolute values:

$$\begin{aligned}
\delta j \;\leq\; & \sum_{n=1}^{n=nmax} \frac{1}{t^{n+1}-t^n} \int_{\Omega_{t^{n+1}}} |\Pi_h W^{*,n+1}||\Pi_h W^{n+1} - W^{n+1}|\,\mathrm{d}\Omega \\
+ & \sum_{n=1}^{n=nmax} \frac{1}{t^{n+1}-t^n} \int_{\Omega_{t^n}} |\Pi_h W^{*,n}||\Pi_h W^n) - W^n|\,\mathrm{d}\Omega \\
+ & \sum_{n=1}^{n=nmax} \int_{\Omega_{t^n}} |\nabla \Pi_h W^{*,n}|\;|\Pi_h \mathcal{F}(W^n) - \mathcal{F}(W^n)|\,\mathrm{d}\Omega \\
+ & \sum_{n=1}^{n=nmax} \int_{\partial\Omega_{t^n}} |\Pi_h W^{*,n}|\;|(\Pi_h \bar{\mathcal{F}}(W^n) - \bar{\mathcal{F}}(W^n)).\mathbf{n}|\,\mathrm{d}\Gamma. \qquad (13)
\end{aligned}$$

5.2 Continuous error model

Working in this framework enables to write Estimate (13) in a *spatially*-continuous form, in which the Π_h are discarded, and in which the interpolation error $Id - \Pi_h$ is replaced by its continuous $Id - \pi_{\mathcal{M}}$. Then, we are interested in minimizing the following

error functional:

$$\begin{aligned}
\mathbf{E}(\mathcal{M}) &= \sum_{n=1}^{n=nmax} \frac{1}{t^{n+1}-t^n} \int_{\Omega_{t^{n+1}}} |W^{*,n+1}||\pi_{\mathcal{M}} W^{n+1} - W^{n+1}| \,\mathrm{d}\Omega \\
&+ \sum_{n=1}^{n=nmax} \frac{1}{t^{n+1}-t^n} \int_{\Omega_{t^n}} |W^{*,n}||\pi_{\mathcal{M}} W^{n} - W^{n}| \,\mathrm{d}\Omega \\
&+ \sum_{n=1}^{n=nmax} \int_{\Omega_{t^n}} |\nabla W^{*,n}| \; |\pi_{\mathcal{M}} \mathcal{F}(W^n) - \mathcal{F}(W^n)| \,\mathrm{d}\Omega \\
&+ \sum_{n=1}^{n=nmax} \int_{\partial\Omega_{t^n}} |W^{*,n}| \, |(\pi_{\mathcal{M}} \bar{\mathcal{F}}(W^n) - \bar{\mathcal{F}}(W^n)).\mathbf{n}| \,\mathrm{d}\Gamma. \qquad (14)
\end{aligned}$$

We observe that the fourth term introduces a dependency of the error with respect to the boundary surface mesh. In the present paper, we discard this term and refer to [12] for a discussion of its influence. The first term can be transformed as follows without introducing a large error:

$$\int_{\Omega_{t^{n+1}}} |W^{*,n+1}||\pi_{\mathcal{M}} W^{n+1} - W^{n+1}| \,\mathrm{d}\Omega = \int_{\Omega_{t^n}} |J_n^{n+1}|^{-1} |\tilde{W}^{*,n+1}||\pi_{\mathcal{M}} \tilde{W}^{n+1} - \tilde{W}^{n+1}| \,\mathrm{d}\Omega$$

where $|J_n^{n+1}|$ is the determinant of the transformation from Ω_n to Ω_{n+1}, and $\tilde{W}^{*,n+1}$ resp. $\tilde{W}^{n+1}$ the functions of Ω_n obtained by reverse transportation from Ω_{n+1}. Then, introducing the continuous interpolation error, we can write the simplified error model as follows:

$$\mathbf{E}(\mathbf{M}) = \sum_{n=1}^{n=nmax} \int_{\Omega} \mathrm{trace}\left(\mathcal{M}^{-\frac{1}{2}}(\mathbf{x}, t^n) \, \mathbf{H}(\mathbf{x}, t^n) \, \mathcal{M}^{-\frac{1}{2}}(\mathbf{x}, t^n) \right) \mathrm{d}\Omega \, \mathrm{d}t$$

with $\mathbf{H}(\mathbf{x}, t^n) = \sum_{j=1}^{5} \mathbf{H}_j(\mathbf{x}, t^n)$, in which

$$\begin{aligned}
\mathbf{H}_j(\mathbf{x}, t^n) &= \frac{1}{t^{n+1}-t^n} \left| |J_n^{n+1}|^{-1} \tilde{W}_j^{*,n+1}(\mathbf{x}, t) \right| \cdot \left| H(\tilde{W}_j^{n+1})(\mathbf{x}) \right| \\
&+ \frac{1}{t^{n+1}-t^n} \left| W_j^{*,n}(\mathbf{x}) \right| \cdot \left| H(W_j^n)(\mathbf{x}, t) \right| \\
&+ \left| \frac{\partial W_j^{*,n}}{\partial x}(\mathbf{x}) \right| \cdot \left| H(\mathcal{F}_1(W_j^n))(\mathbf{x}) \right| + \left| \frac{\partial W_j^{*,n}}{\partial y}(\mathbf{x}) \right| \cdot \left| H(\mathcal{F}_2(W_j^n))(\mathbf{x}) \right| \\
&+ \left| \frac{\partial W_j^{*,n}}{\partial z}(\mathbf{x}) \right| \cdot \left| H(\mathcal{F}_3(W_j^n))(\mathbf{x}) \right| \qquad (15)
\end{aligned}$$

is defined on Ω_n. Here, W_j^* denotes the j^{th} component of the adjoint vector W^*, $H(\mathcal{F}_i(W_j))$ the Hessian of the j^{th} component of the vector $\mathcal{F}_i(W)$, and $H(W_{j,t})$ the Hessian of the j^{th}

component of the time derivative of W. It should be noted that the time derivative can be estimated with more accuracy in order to avoid a large weight $(t^{n+1} - t^n)^{-1}$ which is not compensated due to the rough triangular inequality applied in the above majorations.

5.3 Spatial minimization for a fixed t

Let us assume that at time $t = t^n$, we seek for the optimal continuous mesh $\mathbf{M}_{go}(t)$ which minimizes the instantaneous error, *i.e.,* the spatial error for a fixed time t:

$$\tilde{\mathbf{E}}(\mathbf{M}(t)) = \int_\Omega \text{trace}\left(\mathcal{M}^{-\frac{1}{2}}(\mathbf{x},t)\,\mathbf{H}(\mathbf{x},t)\,\mathcal{M}^{-\frac{1}{2}}(\mathbf{x},t)\right)\,\mathrm{d}\mathbf{x}$$

under the constraint that the number of vertices is prescribed to $\mathcal{C}(\mathcal{M}(t)) = N(t)$. Similarly to [12], solving the optimality conditions provides the *optimal goal-oriented ("go") instantaneous continuous mesh* $\mathcal{M}_{go}(t) = (\mathcal{M}_{go}(\mathbf{x},t))_{\mathbf{x}\in\Omega}$ at time t defined by:

$$\mathcal{M}_{go}(\mathbf{x},t) = N(t)^{\frac{2}{3}}\,\mathcal{M}_{go,1}(\mathbf{x},t)\,, \tag{16}$$

where $\mathcal{M}_{go,1}$ is the optimum for $\mathcal{C}(\mathbf{M}(t)) = 1$:

$$\mathcal{M}_{go,1}(\mathbf{x},t) = \left(\int_\Omega (\det \mathbf{H}(\bar{\mathbf{x}},t))^{\frac{1}{5}}\mathrm{d}\bar{\mathbf{x}}\right)^{-\frac{2}{3}} (\det \mathbf{H}(\mathbf{x},t))^{-\frac{1}{5}}\ \mathbf{H}(\mathbf{x},t). \tag{17}$$

6 CONCLUDING REMARKS

The more complex a model is, the more necessary is the use of a mathematical method in order to control the approximation error. In fluid-structure interaction, a central challenge is the control of the error due to ALE. Several difficulties are combined: (a) the unsteadiness which implies to use several mesh topologies: we have chosen to build the method inside the Transient Fixed point algorithm which freezes the topology during time sub-intervals, (b) mesh motion, for which we use an existing elasticity model, (c) ALE error analysis. This paper concentrates on the (c) issue and proposes a formulation transforming the mesh adaptation problem into a metric-optimization problem. A proper formulation of the state equation is proposed. Several formulations of error paradigms are addressed and transformed into an algorithm involving a well-posed metric-optimization sub-problem. The preliminary results depicted here will be completed for the conference by works in progress dealing with these new formulations.

7 ACKNOWLEDGEMENTS

We thank Geraldine Olivier for fruitful discussions. This work was partly done in the MAIDESC ANR project which is supported by the French ministery of Research under contract ANR-13-MONU-0010.

REFERENCES

[1] F. Alauzet A. Loseille, A. Dervieux. Anisotropic norm-oriented mesh adaptation for compressible flows. In *53rd AIAA Aerospace Sciences Meeting*, 2015.

[2] P.-A. Absil, R. Mahony, and R. Sepulchre. *Optimization Algorithms on Matrix Manifolds*. Princeton University Press, Princeton, NJ, 2008.

[3] F. Alauzet, P.J. Frey, P.L. George, and B. Mohammadi. 3D transient fixed point mesh adaptation for time-dependent problems: Application to CFD simulations. *J. Comp. Phys.*, 222:592–623, 2007.

[4] F. Alauzet and G. Olivier. An L^p-L^∞ space-time anisotropic mesh adaptation strategy for time dependent problems. In *Proceedings of the V ECCOMAS CFD Conf.*, 2010.

[5] F. Alauzet and G. Olivier. Extension of metric-based anisotropic mesh adaptation to time-dependent problems involving moving geometries. In *49th AIAA Aerospace Sciences Meeting and Exhibit*, AIAA-2011-0896, Orlando, FL, USA, Jan 2011.

[6] V. Arsigny, P. Fillard, X. Pennec, and N. Ayache. Log-Euclidean metrics for fast and simple calculus on diffusion tensors. *Magn. Reson. Med.*, 56(2):411–421, 2006.

[7] A. Belme, A. Dervieux, and F. Alauzet. Time accurate anisotropic goal-oriented mesh adaptation for unsteady flows. *J. Comp. Phys.*, 231(19):6323 6348, 2012.

[8] M. Berger. *A panoramic view of Riemannian geometry*. Springer Verlag, Berlin, 2003.

[9] A. Loseille and F. Alauzet. Continuous mesh framework. Part I: well-posed continuous interpolation error. *SIAM J. Numer. Anal.*, 49(1):38–60, 2011.

[10] A. Loseille and F. Alauzet. Continuous mesh framework. Part II: validations and applications. *SIAM J. Numer. Anal.*, 49(1):61–86, 2011.

[11] A. Loseille, A. Dervieux, and F. Alauzet. Fully anisotropic goal-oriented mesh adaptation for 3d steady euler equations. *Journal of Computational Physics*, 229:2866–2897, 2010.

[12] A. Loseille, A. Dervieux, and F. Alauzet. Fully anisotropic goal-oriented mesh adaptation for 3D steady Euler equations. *J. Comp. Phys.*, 229:2866–2897, 2010.

[13] A. Loseille, A. Dervieux, P.J. Frey, and F. Alauzet. Achievement of global second-order mesh convergence for discontinuous flows with adapted unstructured meshes. In *37th AIAA Fluid Dynamics Conference and Exhibit*, AIAA-2007-4186, Miami, FL, USA, Jun 2007.

[14] F. Magoules. *Computational Fluid Dynamics*. CRC Press, Boca Raton, London, New York, Washington D.C., 2011.

[15] D.A. Venditti and D.L. Darmofal. Grid adaptation for functional outputs: application to two-dimensional inviscid flows. *J. Comp. Phys.*, 176(1):40–69, 2002.